Operational Impacts of Wind Generation on California Power Systems

Yuri V. Makarov, *Senior Member, IEEE*, Clyde Loutan, *Senior Member, IEEE*, Jian Ma, *Member, IEEE*, and Phillip de Mello, *Student Member, IEEE*

***Abstract*—The paper analyzes the impact of integrating wind generation on the regulation and load following requirements of the California Independent System Operator (CAISO). These requirements are simulated and compared for the study cases with and without wind generation impacts included into the study for the years 2006 and 2010. Regulation and load following models were built based on hour-ahead and five-minute ahead load and wind generation forecasts. In 2006, the CAISO system peaked at 50 270 MW. Wind generation (at the installed capacity of 2600 MW) had limited impact on the requirement of load following and regulation in the CAISO Balancing Authority. However, in 2010 (with an expected installed capacity of approximately 6700 MW), this impact will significantly increase. The results provide very useful information for the CAISO to adjust its scheduling and real-time dispatch systems to reliably accommodate future wind generation additions within the CAISO Balancing Authority.**

***Index Terms*—Capacity, load following, load forecast, ramp rates, real-time dispatching, regulation, scheduling, swinging door algorithm, wind generation forecast, wind power.**

I. Introduction

WIND power is an important renewable energy resource in California. Installed wind capacity in California is rapidly growing, and is becoming an important component of the future power generation portfolio. To further develop renewable power, the state enacted a Renewable Portfolio Standard (RPS) requiring each retail seller of energy to procure 20% of its customer sales from renewable energy resources by December 31, 2010.

Over the last decade, researchers have made significant effort to evaluate the impact of wind generation on the operations and cost of power grids. Grubb [1] addressed the integration of renewable energy into large power system. Hatziargyriou and Zervos [2] described more recent state and prospects of wind power in Europe. Parsons *et al.* [3] and Smith [4] presented comprehensive reviews on the wind impacts on the U.S. power grid.

Many researchers have addressed more detailed studies on the impacts of wind generation on the operation of power systems of different nations [5]–[12]. Strbac *et al.* [13] assessed the costs and benefits of wind generation on the U.K. electricity system based on assumed different levels of wind power capacity. In a study on the potential impact of wind generation on the load following capability of a medium-sized power system, Persaud *et al.* [14] found that the magnitudes of power output fluctuations from well-dispersed wind farms are small compared to system demand variations. Consequently, a conclusion was made that wind power expansion would not impose significant additional load following duty on the power system. Persaud *et al.*[15] studied the potential impact of significant wind power capacity on generator loading levels, system reserve availability and generator ramping requirements, and found that wind power generation did not significantly increase the ramping duty on the studied system. Ummels *et al.* [16] investigated the technical capabilities of a thermal generation system for balancing wind power by taking into account ramp-rate constraints. Sørensen [17] studied the wind integration on ramp rates of power grid, focusing on the ramping characteristics of the wind farm at different power levels. Holttinen [18] estimated the increase in hourly load-following reserve requirements based on real wind power production and synchronous hourly load data in the four Nordic countries. The result demonstrated an increasing effect on reserve requirements with increasing wind power penetration. In [19], Ummels *et al.* presented balancing generation/load imbalances and their implications on the Dutch power system integration of wind power. Kirby and Hirst [20] discussed the economic efficiency and equity benefits of assessing charges on the basis of customer-specific costs, focusing on regulation and load following, and determined the extent to which individual customers and groups of customers contribute to the system's generation requirements for these two services.

Generally, these studies used sequential time-series to model and forecast the wind and load behaviors followed by extensive statistical analyses to characterize the wind and load variability. In some studies, such as [21], detailed modeling of ancillary service deployments was performed to determine both the amount of ancillary service required to be procured as a function of wind penetration, and to assess the suitability of procurement procedures. Then, system-wide power production simulation was performed to determine the system's ability to provide ancillary services and associated costs of these services [21].

From California's perspective, the California Energy Commission (CEC) studied the impacts of all types of renewable resources on the power system. Their examination of wind power effects included only modest increases in load following and regulation requirements [22], [23]. In a study conducted inter-

Manuscript received March 27, 2008; revised August 25, 2008. First published March 31, 2009; current version published April 22, 2009. Paper no. TPWRS-00229-2008.

Y. V. Makarov and J. Ma are with Pacific Northwest National Laboratory (PNNL, operated by Battelle), Richland, WA 99354 USA (e-mail: yuri.makarov@pnl.gov; jian.ma@pnl.gov).

C. Loutan and P. de Mello are with California Independent System Operator (California ISO), Folsom, CA 95630 USA (e-mail: cloutan@caiso.com; pdemello@caiso.com).

Color versions of one or more of the figures in this paper are available online at http://ieeexplore.ieee.org.

Digital Object Identifier 10.1109/TPWRS.2009.2016364

0885-8950/$25.00 © 2009 IEEE

Authorized licensed use limited to: Chris Mensah-Bonsu. Downloaded on April 29, 2009 at 12:58 from IEEE Xplore. Restrictions apply.

nally by the CAISO [24] using a mathematical model of the CAISO operations and market, it found that the wind generation had a considerable impact on the regulation and load following requirements. A disadvantage of this former study is that it was oriented to the previous CAISO operational and market systems that included manual real-time dispatch. The former study did not simulate an advanced wind generation forecasting service and was not capable of evaluating the future wind generation impacts. These drawbacks have been overcome in this study. Since then a major reorganization of the CAISO market system has been undertaken. The CAISO operates a two settlement market structure, a day-ahead market which allows parties to bid and schedule load and generation for the following day and a real-time market which clears supply and demand on a five-minute basis to meet current system conditions. A third piece of the market structure is the hour-ahead scheduling process (HASP) which allows parties to submit further bids, clears congestion, and issues advisory schedules and prices but does not have a formal settlement [25]. The CAISO Participating Intermittent Resource Program (PIRP) [26], [27] includes a mandatory day-ahead and hour-ahead forecast service for participating resources. It is expected that new wind generation projects will opt to join the PIRP.

The subsequent sections of this paper describe a detailed methodology to determine the amount of regulation and load following capability needed in the CAISO Balancing Authority. Minute-to-minute variations and statistical interactions of the system parameters of wind generation and load forecast involved in actual scheduling, real-time dispatch, and regulation processes are modeled with sufficient details to mimic the actual CAISO operating practice to provide a robust and accurate assessment of the additional load following and regulation capacity, as well as ramp rate and duration requirements caused by the integration of wind generation in the CAISO's Automatic Generation Control (AGC) and load following Automated Dispatch System (ADS) systems. The expected wind profile in 2010 was developed by AWS Truewind, while the expected load demand was scaled up using actual 2006 load data. Load and wind forecast errors observed in 2006 were then added to the expected load and wind profiles for 2010 to determine the forward schedules. Simulations mimicking the CAISO market timelines with and without wind generation were done to determine the load following and regulation requirements due to wind. The proposed methodology can be used by balancing authorities, utilities, project developments and government organization (RPS developers) to evaluate more accurately the impact of wind generation impacts on the grid balancing generation requirements.

This paper is organized as follows. In Section II, the basic concepts of CAISO real-time and hour-ahead dispatch are described. In Section III, the methodology applied by the CAISO to model load and wind generation forecast errors is presented. Load following and regulation assessment, and ramping requirements assessment are presented in Section IV. The method to forecast hour-ahead and real-time load and wind generation are described in Section V. The stochastic behavior of the variable load models and wind resources are presented in this section. In Section VI, simulation results are presented and analyzed. Conclusion remarks and a discussion of the implications of the results are presented in Section VII.

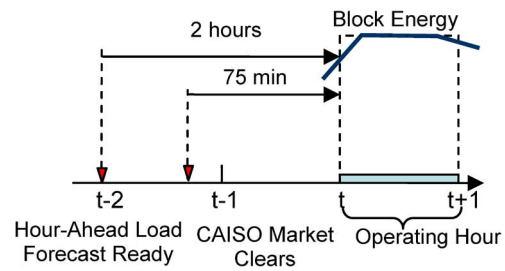

Fig. 1. CAISO hour-ahead scheduling timeline.

II. CAISO Scheduling and Real-Time Basics and Timelines

The methodology developed to analyze the wind generation impacts is based on a mathematical model of the CAISO's actual scheduling, real-time dispatch, and regulation processes and their timelines. Minute-to-minute variations and statistical interactions of the system parameters involved in these processes are depicted with sufficient details to provide a robust and accurate assessment of the additional regulation and load following capacity, ramping and ramp duration requirements that the CAISO Balancing Authority is expected to face with higher penetration of wind generation.

A. Generators' Schedules

Hour-ahead schedules are hourly block energy schedules including the 20-min ramps between hours (Fig. 1). They are provided 75 min before the actual beginning of an operating hour.

The load forecast used for the hour-ahead scheduling process is provided 2 h before the beginning of an operating hour. The difference between the day-ahead and hour-ahead schedules constitutes the required generation adjustment. The CAISO facilitates the adjustment bids and the market.

Load following is an instructed deviation from schedule caused by the real-time (or supplemental) energy dispatch. The desired changes of generation are determined in real-time for each 5-min dispatch interval. Fig. 2 illustrates how the generators in the CAISO Balancing Authority are scheduled and dispatched.

B. Real-Time Dispatch and Regulation

Under normal operating conditions, supply and demand in a power grid must always remain balanced. In real-time, generators under automatic generation control are adjusted to match any variation in demand. Generally the variations in generation and demand are difficult to predict, therefore, the system dispatchers need appropriate automatic response and reserves to deal with rapid and slow variations from a few minutes to several hours.

The real-time dispatch is automatically conducted by the CAISO's MRTU applications using 15-min intervals for unit commitment and 5-min interval for economic dispatch. Fig. 3 illustrates the timeline for this process. The desired changes of generation are determined in real-time for each 5-min dispatch interval 5 min before the actual beginning of the interval.

Authorized licensed use limited to: Chris Mensah-Bonsu. Downloaded on April 29, 2009 at 12:58 from IEEE Xplore. Restrictions apply.

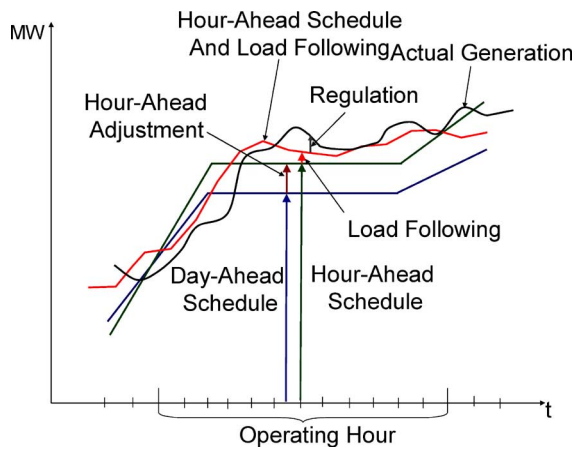

Fig. 2. Typical CAISO hourly scheduling and real-time requirement.

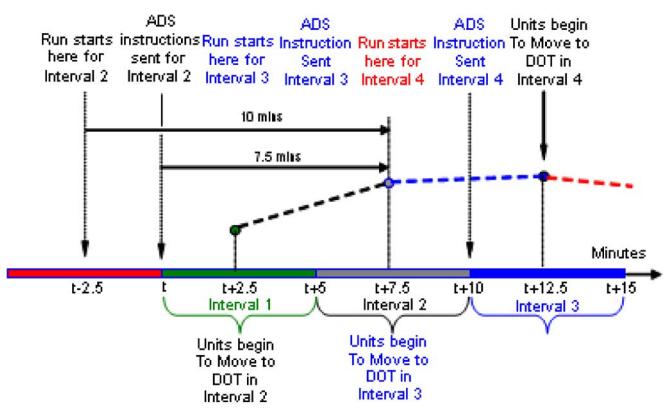

Fig. 3. CAISO real-time dispatch timeline.

System information used for that purpose is dated back 7.5 min before the beginning of the interval. Units start to move toward the new set point 2.5 min before the interval begins. They are required to reach the set point in the middle of the interval (2.5 min after its beginning). The units may ramp by sequential segments, that is, the ramp is not necessarily constant.

The CAISO utilizes a Very Short Term Load Predictor (VSTLP) program to provide an average load forecast for the interval $[\mathrm{t}, \mathrm{t}+5]$ 7.5 min before the beginning of the interval or 10 min before the middle point of this interval. The VSTLP program uses real-time telemetry data to generate the forecast.

For wind generation in the PIRP, the wind forecasts are provided by a forecast service provider. Scheduling errors and variability of wind generation is balanced in real-time by the CAISO. The net deviations from schedule for wind is then settled at an average price, reducing penalties for inherent variability.

III. Methodology Applied by the CAISO

In this section, the methodology used by the CAISO to model load forecast errors and wind generation forecast errors is described. The wind generation and load data used in the statistical analysis is actual wind generation and load data realized in the CAISO system in 2006.

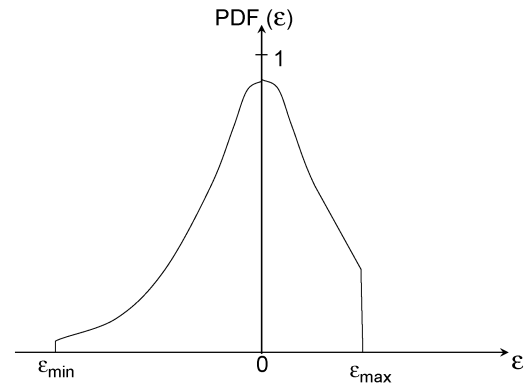

Fig. 4. Doubly truncated normal distribution.

A. Random Number Generator Based on Truncated Normal Distribution

One important task of the study was to generate realistic load forecast errors. The assumption used in this paper is that the distribution of hour-ahead forecast errors is an unbiased truncated normal distribution (TND). This is based on the fact that the values of a normally distributed random variable can, in theory, assume any value over the range from $-\infty$ to $+\infty$ which may lead to significant computational errors in situations where the distribution's outcomes are constrained. Meanwhile, the characteristic parameters (i.e., mean ε_0 and standard deviation σ) of truncated normal distributions can be readily derived using basic statistical methods.

The probability density function (PDF) of the doubly truncated normal distribution (shown in Fig. 4) is expressed by the following formula:

$$PDF_{TND}(\varepsilon) = \begin{cases} 0, & -\infty \le \varepsilon < \varepsilon_{\min} \\ PDF_N(\varepsilon), & \varepsilon_{\min} \le \varepsilon < \varepsilon_{\max} \\ 0, & \varepsilon_{\max} \le \varepsilon < +\infty \end{cases} \quad (1)$$

where $\varepsilon_{\min}$ and $\varepsilon_{\max}$ are the lower and the upper truncation points, respectively, and $PDF_N(\varepsilon)$ denotes the PDF of the standard normal distribution, which can be specified as

$$PDF_N(\varepsilon) = \frac{1}{\sqrt{2\pi\sigma^2}} e^{-\frac{1}{2}\left(\frac{\varepsilon-\varepsilon_0}{\sigma}\right)^2}, \quad -\infty \le \varepsilon \le +\infty \quad (2)$$

where ε_0 refers to mean and σ is standard deviation. Fig. 5 illustrates the actual PDF and the normal distribution PDF of hour-ahead load forecast error distribution for 2006.

B. Load Forecast Errors

The load is modeled as a stochastic quantity, represented by two series of minute-to-minute values: the load average value and its standard deviation magnitude. Hour-ahead hourly load forecast is provided by the CAISO's Automated Load Forecasting System 120 min before the operating hour begins. The hour-ahead load forecast error is the difference between the average actual load over an operating hour and the hour-ahead load schedule (Fig. 6). This error is denoted as $\varepsilon_{L,ha}$ (see Fig. 7). The hypothesis concerning the TND distribution of $\varepsilon_{L,ha}$ is

Authorized licensed use limited to: Chris Mensah-Bonsu. Downloaded on April 29, 2009 at 12:58 from IEEE Xplore. Restrictions apply.

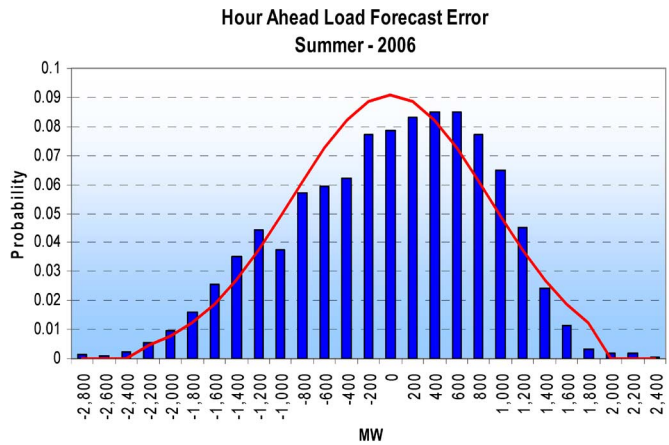

Fig. 5. Hour-ahead load forecast error distribution for Summer 2006 (actual PDF versus the normal distribution PDF).

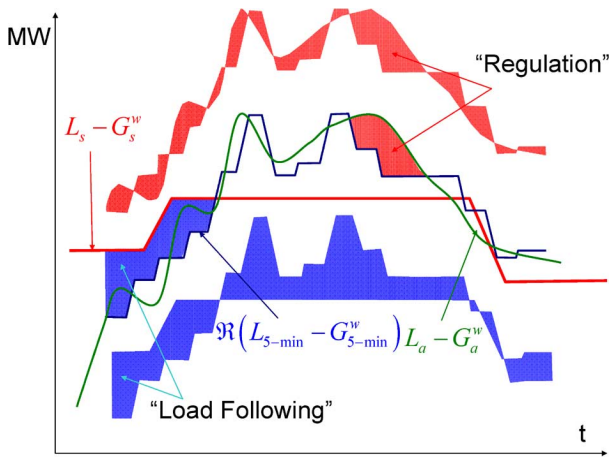

Fig. 6. Separation of regulation from load following based on simulated hour-ahead schedule.

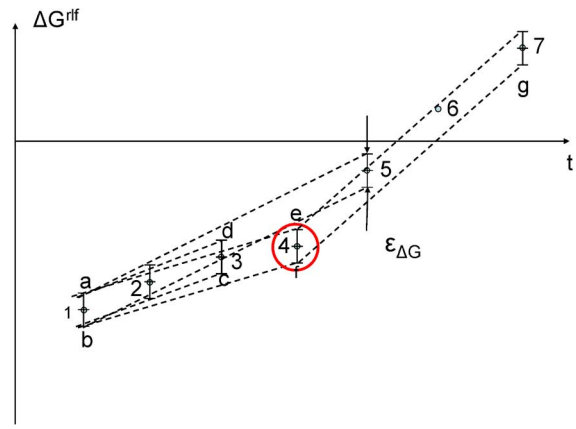

Fig. 7. Concept of the "swinging window" algorithm.

TABLE I
HOUR-AHEAD LOAD FORECAST ERROR CHARACTERISTICS FOR 2006 (IN MW)

Seasons	Winter	Spring	Summer	Fall
Average	-22.49	-24.05	-130.43	-69.21
Min	-2680.12	-2101.08	-3770.73	-2627.90
Max	1842.06	1930.54	2446.12	2080.98
Std. Dev.	637.37	601.34	900.13	687.52
Autocorrelation	0.70	0.73	0.89	0.83

TABLE II
REAL-TIME LOAD FORECAST ERROR CHARACTERISTICS (IN MW)

Average	1.1
Minimum	-349.5
Maximum	349.4
Std. Dev.	97.8
Autocorrelation	0.6

TABLE III
ESTIMATED HOUR-AHEAD WIND GENERATION FORECAST CHARACTERISTICS (IN FRACTION OF CAPACITY)

Seasons	Winter	Spring	Summer	Fall
Average	0.00012	-0.0005	-0.00047	0.00058
Minimum	-0.35678	-0.43313	-0.32185	-0.31930
Maximum	0.30918	0.30840	0.30742	0.39663
Std. Dev.	0.07233	0.08987	0.07955	0.07922
Autocorrelation	0.61062	0.70609	0.65185	0.59392

confirmed by the analysis of the actual hour-ahead error provided in Fig. 5. The mean absolute percent error (MAPE) of the hour-ahead load forecast stays within 2% of the peak load.

After analysis, average, maximum, minimum values and standard deviation of the relevant variables are obtained. These values are used to represent the proposed operation strategy for the load forecast errors. Table I shows the standard deviation and autocorrelation of the hour-ahead load forecast error $\sigma_{L,ha}$ for the year 2006. It is assumed that the same statistical characteristics of the hour-ahead load forecast error will be observed in the year 2010, including autocorrelation.

It was also assumed that the same statistical characteristics of the real-time load forecast error will be observed in the year 2010. The standard deviation and autocorrelation of the real-time load forecast error $\sigma_{L,rtf}$ is set to values shown in Table II. All seasons of real-time load forecasts use the same error statistics in MW.

C. Actual Wind Generation Forecast Errors Observed in 2006

Similar to load, the available wind generation forecast error is assumed to be a TND quantity, represented by two series of hourly values: the wind-power average error value (zero) and its standard deviation. The hour-ahead wind generation forecast will be a part of the future CAISO scheduling system. It is assumed that the 2-h-ahead wind generation forecast error is distributed according to the TND law with the characteristics shown in Table III, derived from 2006 wind generation forecast data.

IV. ASSESSMENT OF REGULATION AND LOAD FOLLOWING IMPACTS

A. Area Control Error

The CAISO's operation control objective is to minimize its area control error (ACE) to the extent sufficient to comply with the NERC Control Performance Standards [28]. Therefore, the

Authorized licensed use limited to: Chris Mensah-Bonsu. Downloaded on April 29, 2009 at 12:58 from IEEE Xplore. Restrictions apply.

"ideal" regulation/load following signal is the signal that opposes deviations of ACE from zero when it exceeds a certain threshold:

$$\begin{aligned} -ACE &= -(I_a - I_s) + \underbrace{10B(F_a - F_s)}_{Neglected} \\ &\approx G_s - L_s - G_a + L_a \rightarrow \min \end{aligned} \tag{3}$$

where I_a denotes net interchange (MW flow out of the Balancing Authority); I_s refers to scheduled net interchange; B is area frequency bias constant; F_a and F_s are actual and scheduled frequency, respectively. Impacts of wind generation on the interconnection frequency are neglected. This is a valid assumption given the large interconnection (>140 GW peak load) whose frequency deviates by very small amounts with normal imbalances and which is maintained by several balancing authorities. The generation component of the ACE equation can be represented as follows:

$$G_s = G_{ha} + G_{ha}^w \tag{4}$$

$$G_a = G_s + \Delta G^{lf} + \Delta G^r + \Delta G^w + \Delta G^{ud} \tag{5}$$

where ha denotes the hour-ahead generation schedule; lf denotes instructed deviations from the hour-ahead schedule caused by generators involved into the load following process; r denotes instructed deviations caused by generators involved into the regulation process; ΔG^{lf} and ΔG^r are the deviations of the regulation and load following units from their base points; ΔG^w is the deviation of the wind generators from their schedule (wind generation real-time schedule forecast error); and ΔG^{ud} is the total deviation of generators from the dispatched instructions. ΔG^{ud} is simulated similarly to the load forecast error (random number generator based on TND).

The total deviation of generators from dispatch instructions for the conventional units that are not involved in regulation and load following can be represented as follows:

$$\Delta G^{ud} = G_a - G_{ha} \tag{6}$$

$$\Delta G^w = G_a^w - G_{ha}^w \tag{7}$$

$$\Delta L = L_a - L_{ha}. \tag{8}$$

Since the control objective is $ACE \rightarrow 0$, (3) can be rewritten as

$$\Delta G^{lf} + \Delta G^r = \Delta L - \Delta G^w - \Delta G^{ud} \tag{9}$$

where ΔL is the deviation of the actual load from its real-time scheduled value (load forecast error).

Equation (9) is written for instantaneous values of ΔL, ΔG^w, and ΔG^{ud}. Therefore, the statistical interaction between the load forecast error and the wind generation forecast error is fully preserved in (9). The load and wind generation errors can vary depending on the wind generation penetration level within the CAISO Balancing Authority and the accuracy of the load forecast compared to the accuracy of the wind generation forecast. Since the percent wind generation forecast error is more significant than the percent load forecast error, the former may have a considerable impact on $\Delta G^{lf} + \Delta G^r$.

Wind generation would have no impact on regulation and load following requirements if

$$\Delta G^w = 0. \tag{10}$$

By substituting (10) into (9), we have

$$\Delta G^{rlf} = \Delta G^{lf} + \Delta G^r = \Delta L - \Delta G^{ud}. \tag{11}$$

B. Load Following and Regulation Assessment

Load following is understood as the difference between the hourly energy schedule including 20-min ramps (in Fig. 6) and the short-term 5-minute forecast/schedule and applied "limited ramping capability" function. This difference is also shown as the blue area below the curves. *Regulation* is interpreted as the difference between the actual CAISO generation requirement and the short-term 5-min dispatch shown in Fig. 6 as the red area between the blue and green lines.

The hour-ahead and 5-min schedules for load and hour-ahead schedule for wind generation are generated using forecast errors observed in 2006. Then regulation was separated from load following. The schedule/forecast based approach uses the short-term forecasts of wind generation and load, $G_{rtf,5\min}^{w,y}$ and $L_{rtf,5\min}^{y}$. In this case, the following formulas can be used:

$$\begin{aligned} \Delta G^r(m) = {} & L_a^y(m) - G_a^{w,y}(m) - L_{rtf,5\min}^y(m) \\ & + G_{rtf,5\min}^{w,y}(m) \end{aligned} \tag{12}$$

$$\begin{aligned} \Delta G^{lf}(m) = {} & L_{rtf.5\min}^y(m) - G_{rtf,5\min}^{w,y}(m) - L_{rtf,1hr}^y(m) \\ & + G_{ha,1hr}^{w,y}(m). \end{aligned} \tag{13}$$

C. Assessment of Ramping Requirements

The regulating unit ramping capability can directly influence the required regulation and load following capacity. If the ramping capability is insufficient, more units and more capacity must be involved in regulation to follow the ramps. Hence, a simultaneous evaluation is necessary to determine the true requirements.

The required ramping capability can be derived from the shape of the regulation/load following curve ΔG^{rlf}. This derivation needs to be done in a scientific way. We propose to use the "swinging window" algorithm [29] for this purpose. This is a proven technical solution implemented in the PI Historian and widely used to compress and store time dependent datasets.

Fig. 7 demonstrates the concept of the "swinging window" approach. A point is classified as a "turning point" whenever for the next point in the sequence any intermediate point falls out of the admissible accuracy range $\pm\varepsilon_{\Delta G}$. For instance, for point 3, one can see that point 2 stays inside the window $abcd$. For point 4, both points 2 and 3 stay within the window $abef$.

Authorized licensed use limited to: Chris Mensah-Bonsu. Downloaded on April 29, 2009 at 12:58 from IEEE Xplore. Restrictions apply.

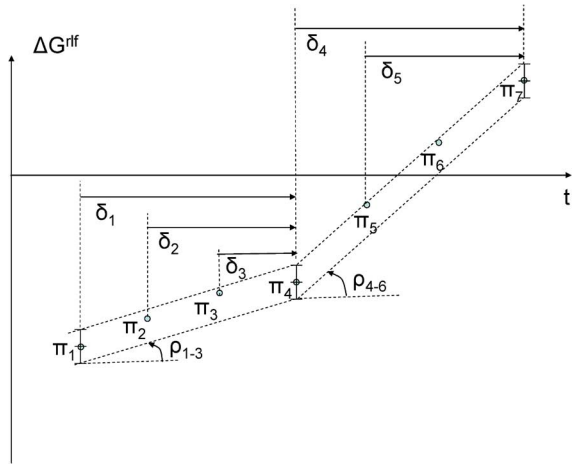

Fig. 8. "Swinging window" algorithm—obtaining regulation, ramps, and ramp duration.

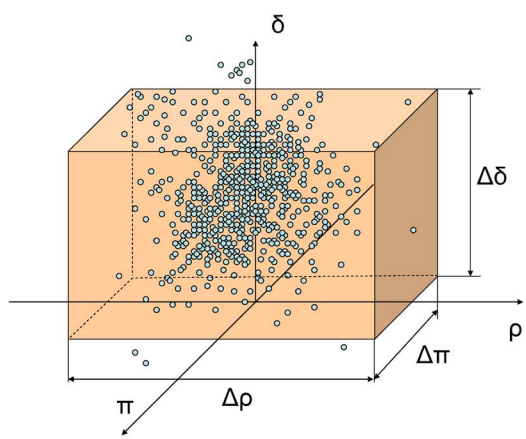

Fig. 9. Concurrent consideration of the capacity, ramping, and duration requirements.

But for point 5, point 4 goes beyond the window, and therefore point 4 is marked as a turning point.

In this analysis, points 1, 2, and 3 correspond to the different magnitudes of the regulation signal, π_1, π_2, and π_3, whereas the ramping requirement at all these points is the same, ρ_{1-3} (see Fig. 8). The swinging door algorithm also helps to determine the ramp duration δ.

D. Concurrent Statistical Analysis of the Regulation and Load Following Requirements

As it has been discussed before, the regulation capacity and ramping requirements are inherently related. Insufficient ramping capability could cause additional capacity requirements. In this paper, we propose to apply a multivariable statistical analysis to provide a concurrent consideration of the regulation and load following capacity, ramping and ramp duration requirements.

For the regulation/load following requirement curve ΔG^{rtf}, we can apply the "swinging window" algorithm and determine the sequences of its magnitudes and ramps, $\pi_1, \pi_2, \ldots$, $\rho_1, \rho_2, \ldots$, and $\delta_1, \delta_2, \ldots$. The triads $(\pi_{\mathrm{i}}, \rho_{\mathrm{i},}, \delta_{\mathrm{i}})$ can be used to populate the three-dimensional space of these parameters (see Fig. 9).

For given ranges of these three parameters, $\Delta\pi$, $\Delta\rho$, and $\Delta\delta$, a box can be plotted in this space, so that some triads are inside the box (N_{in}), some are outside (N_{out}). This approach helps to determine the probability of being outside the box

$$p_{out} = \frac{N_{out}}{N_{out} + N_{in}}. \tag{14}$$

If a point lies outside the box, the regulation/load following requirements are not met at this point. We will require that this probability must be below certain minimum probability, $P_{\min}$. The purpose is to find the position of the wall of the probability box that corresponds to a given $P_{\min}$.

V. Simulation of Future Scenarios and Data Set Generation

This section provides a detailed description of the applied modeling techniques for describing the stochastic behavior of the driving variables, i.e., hour-ahead and real-time load forecast and wind generation forecast error.

A. Actual Load

For a future study year $2006+i$, the actual annual load curve can be simulated as the year 2006 load multiplied by the ith power of the annual load growth factor

$$L_a^{2006+i} = (1+\gamma)^i \times L_a^{2006}. \tag{15}$$

The actual one-minute resolution load data are used for this study. The annual growth factor i is set as 1.5%.

B. Hour-Ahead Load Schedule Model

The scheduled load is the one-hour block energy schedule that includes 20-min ramps between the hours (Fig. 10). It is calculated based on the load forecast error using the following approach. The hour-ahead load schedule $L_{ha,1\ \mathrm{hr}}^{2006+i}$ is simulated based on the projected actual load (15) and the expected load forecast error $\varepsilon_{L,ha}$

$$L_{ha,1hr}^{2006+i} = \Re_{20}\left\{avg_{1hr}\left(L_a^{2006+i}\right) - \varepsilon_{L,ha}\right\} \tag{16}$$

where $\varepsilon_{L,ha}^{\min} \leq \varepsilon_{L,ha} \leq \varepsilon_{L,ha}^{\max}$, $\varepsilon_{L,ha}^{\max} = 3\sigma_{L,ha}$, and $\varepsilon_{L,ha}^{\min} = -3\sigma_{L,ha}$; and the operator $\Re_{20}$ adds 20-min linear ramps to the block energy load schedule.

The hour-ahead load schedule is simulated using a TND random number generator based on the statistical characteristics of the load forecast error (derived from 2006 and 2007 data evaluated by the CAISO; see Table I). The error distribution applied to the hour-ahead schedule is shown in Fig. 11.

Based on these specified values, a random number generator is used to generate values of $\varepsilon_{L,ha}$ with the PDF function determined by (1). For each operating hour, the random values of $\varepsilon_{L,ha}$ are substituted into (16) to produce the simulated hour-ahead load schedule. It is assumed that the load

Authorized licensed use limited to: Chris Mensah-Bonsu. Downloaded on April 29, 2009 at 12:58 from IEEE Xplore. Restrictions apply.

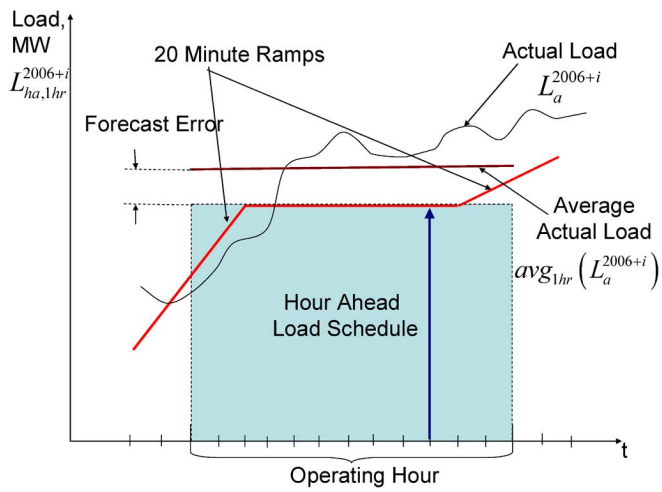

Fig. 10. CAISO simulated hour-ahead load schedule (red line).

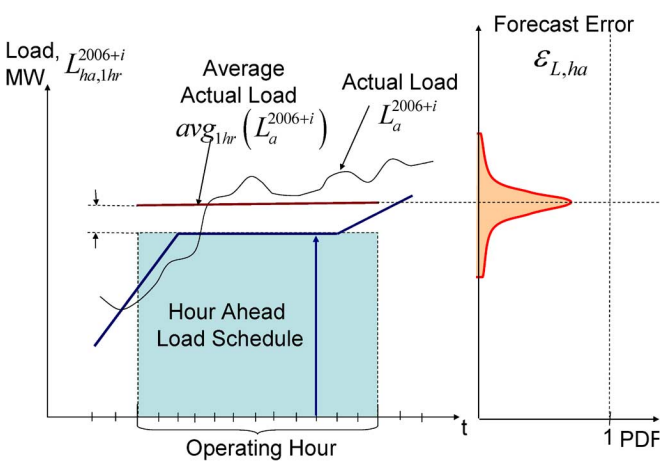

Fig. 11. Probability density function (PDF) of the load forecast function (red line).

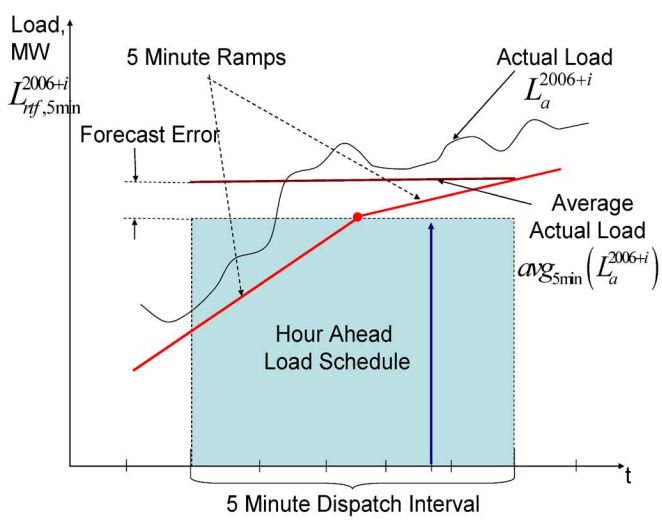

Fig. 12. CAISO simulated real-time load forecast (red line).

error distribution is *unbiased* for $PDF_N(\varepsilon)$, that is $\varepsilon_0 = 0$, and $\varepsilon^{\min}_{L,ha}, \varepsilon^{\max}_{L,ha}$ correspond to the minimum and maximum forecast errors specified for this study. Based on the above approach, hour-ahead load scheduling was simulated for each season of 2006 and 2010.

C. Real-Time Load Forecast

The real-time load forecast is the average 5-min load forecast that includes 5-min ramps between the hours (shown in Fig. 12). The real-time load forecast $L^{2006+i}_{rtf,5\,\min}$ is simulated based on the projected actual load (15) and the expected load forecast error $\varepsilon_{L,rtf}$

$$L^{2006+i}_{rtf,5\,\min} = \Re_5\left\{avg_{5\,\min} L^{2006+i}_{a} - \varepsilon_{L,rtf}\right\} \tag{17}$$

where $\varepsilon^{\min}_{L,rtf} \leq \varepsilon_{L,rtf} \leq \varepsilon^{\max}_{L,rtf}$, $\varepsilon^{\max}_{L,rtf} = 3\sigma_{L,rtf}$, and $\varepsilon^{\min}_{L,rtf} = -3\sigma_{L,rtf}$; and the operator $\Re_5$ adds 5-min ramps to the block energy load schedule.

The real-time load forecast is simulated using a random number generator based on the statistical characteristics of the real-time load forecast error (derived from 2006 and 2007 data evaluated by the CAISO; see Table II). The suggested probability distribution for the real-time load forecast error is unbiased doubly truncated normal distribution. The values of $\varepsilon^{\min}_{L,rtf}$ and $\varepsilon^{\max}_{L,rtf}$ are set to plus/minus $3\sigma_{L,rtf}$. The standard deviation of the real-time load forecast error $\sigma_{L,rtf}$ is set as shown in Table II. Based on these specified values, a random number generator will be used to generate values of $\varepsilon_{L,rtf}$. For each operating hour, the random values of $\varepsilon_{L,rtf}$ will be substituted into (17) to produce the simulated real-time load forecast.

D. Wind Generation Hour-Ahead Scheduling Model

The ability to forecast wind power output in both hourly and day-ahead time frames is often an overlooked key factor [3]. Reliable wind data are essential for a detailed wind assessment. Wind generation data was developed by combining a previous energy output scenario with the short term variability from current wind plants.

Wind generation hour-ahead schedules are simulated using the wind generation year 2010 model described above and wind generation forecast error model described below. Similar to the load hour-ahead schedule and real-time load forecast models, the wind generation schedules and forecasts can be simulated for the hour-ahead scheduling and real-time dispatch time horizons as follow:

Wind generation schedule model $G^{w}_{ha,1\ \mathrm{hr}}$ for the real-time scheduling process (hourly block energy forecast schedule) is as follows:

$$G^{w,2006+i}_{ha,1hr} = \Re_{20}\left\{avg_{1hr}\left(G^{w,2006+i}_{a}\right) - \varepsilon_{w,ha}\cdot CAP^{w,2006+i}\right\}. \tag{18}$$

The wind generation forecast error is expressed in percent of the wind generation capacity, $CAP^{w,2006+i}$. Operator $\Re_{20}\{\ldots\}$ adds 20-min ramps between the hours; $\varepsilon_{w,ha}$ is the simulated hour-ahead wind generation forecast error. This error is generated with the help of *unbiased* TND random number generator. The TND has the following characteristics: 1) Parameters $\varepsilon^{\min}_{w,ha}$, $\varepsilon^{\max}_{w,ha}$ correspond to the minimum and maximum total CAISO wind generation forecast errors

Authorized licensed use limited to: Chris Mensah-Bonsu. Downloaded on April 29, 2009 at 12:58 from IEEE Xplore. Restrictions apply.

specified for the TND. These values are set to plus/minus 3 standard deviation of the hour-ahead wind generation forecast error $\sigma_{w,ha}$; 2) The standard deviation and autocorrelation of the hour-ahead wind generation forecast error $\sigma_{w,ha}$ is set to the seasonal values provided in Table I.

The truncation process is based on the following rules:

$$G_{ha,1hr}^{w,2006+i} = avg_{1hr}\left(G_a^{w,2006+i} - \varepsilon_{w,ha} \cdot CAP^{w,2006+i}\right) \tag{19}$$

where $\varepsilon_{w,ha}^{\min} \leq \varepsilon_{w,ha} \leq \varepsilon_{w,ha}^{\max}$. $\varepsilon_{w,ha}^{\min}$ and $\varepsilon_{w,ha}^{\max}$ can be determined by the methodin (20) and (21) at the bottom of the page, where $Index_{\min} = avg_{1\text{ hr}}(G_a^{w,2006+i}) + 3\sigma_{w,ha} \cdot CAP^{w,2006+i}$ and $Index_{\max} = avg_{1\text{ hr}}(G_a^{w,2006+i}) - 3\sigma_{w,ha} \cdot CAP^{w,2006+i}$.

E. Wind Generation Real-Time Scheduling Model

Real-time wind generation forecast is not provided or included into the real-time dispatch process. It is assumed that the naïve persistence model [30] is implicitly used. The real-time 5-min load forecasts are provided 7.5 min before the actual beginning of a 5-min dispatch interval (or 10 min before the middle point of this interval). This means that for a 5-min dispatch interval $[t, t+5]$, the implicit real-time wind generation forecast $G_{rtf,5\text{ min}}^{w,2006+i}$ is assumed to be equal to the actual wind generation at the moment $t-8$

$$G_{rtf,5\text{ min}}^{w,2006+i}[t, t+5] = G_a^{w}[t-8]. \tag{22}$$

Persistence or naïve predictor is a very simple, but yet relatively effective model to forecast wind generation near real time. The persistence forecast model requires time series of measured wind power as input [30].

VI. Simulation Results

The CAISO actual 2006 data and the simulated 2010 data are broken down into the four seasons and then analyzed. Monte Carlo simulations are used to generate sufficient numbers of load following and regulation requirements for each season of 2006 and 2010. The operational analysis focused on integrating a total of approximately 6700 MW of wind generation in 2010 (~2600 MW existing with a peak load of 50 GW in 2006 and ~4100 MW new in 2010). Both load following and regulation requirements analysis, including the capacity, ramping, and duration requirements by operating hour within a season of 2006 and 2010 are conducted. For each analysis, results "with wind" were compared with the corresponding results "without wind."

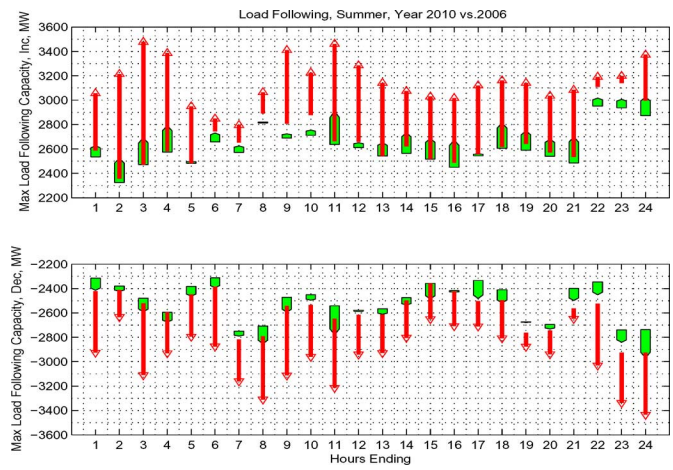

Fig. 13. Hourly capacity diagrams for load following scenarios with wind and without wind in 2006 and 2010.

Only the results for the summer season are presented in this section for illustration.

A series of data of one season of the year were treated as a round of simulation. Then the maximum number of load following or regulation capacity in each hour for all days in a season was found by statistical method. These maximum numbers for each hour in the cases of with and without wind are treated as the target data shown in the Figs. 13, 14, 16, and 17. The "swinging window" algorithm was applied to the simulated load following and regulation data to obtained triplets of regulation, ramp rate and duration. Then the concurrent statistical analysis method described in Section IV-D is applied to the triplet groups of regulation and load following requirements to obtained duration-ramp rate diagrams (Figs. 15 and 18).

All the models described above were implemented in MATLAB codes. All simulations were conducted on a DELL Precision Workstation 370, with an Intel(R) Pentium(R) 4 CPU of 3.4 GHz. The computer is equipped with 1024 MB total physical memory and 2 GB total virtual memory. The operating system is Windows XP Professional (SP2), and the simulation platform is MATLAB 7.4.0 (R2007a).

A. Load Following Requirement

Fig. 13 shows hourly capacity requirements for load following "with wind" and "without wind" for 2006 and 2010. The impact of wind generation on load following for each hour is plotted. The upper part of the diagram shows the maximum load following capacity increase in MW while the maximum capacity decrease is shown in the lower part of diagram. The wider arrows show the load following capacity for each hour

$$\varepsilon_{w,ha}^{\min} = \begin{cases} 3\sigma_{w,ha}, & \text{if} \quad Index_{\min} < CAP^{w,2006+i} \\ avg_{1hr}\left(G_a^{w,2006+i}\right), & \text{if} \quad Index_{\min} \geq CAP^{w,2006+i} \end{cases} \tag{20}$$

$$\varepsilon_{w,ha}^{\max} = \begin{cases} 3\sigma_{w,ha}, & \text{if} \quad Index_{\max} > 0 \\ avg_{1hr}\left(G_a^{w,2006+i}\right), & \text{if} \quad Index_{\max} \leq 0 \end{cases} \tag{21}$$

Authorized licensed use limited to: Chris Mensah-Bonsu. Downloaded on April 29, 2009 at 12:58 from IEEE Xplore. Restrictions apply.

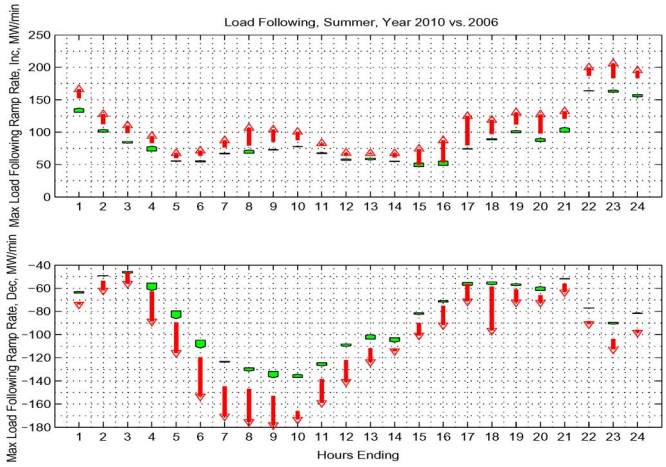

Fig. 14. Hourly ramp rate diagrams for load following scenarios with wind and without wind in 2006 and 2010.

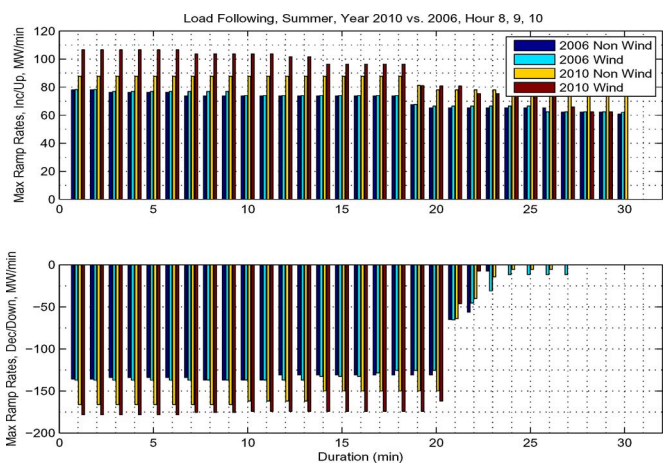

Fig. 15. Duration—ramp rates for load following scenario (hour ending by 8, 9, and 10) with wind and without wind in 2006 and 2010.

in 2006, and the thinner arrows denote load following capacity for 2010. The tail of each arrow represents the load following capacity requirement "without wind," and the tip of each arrow shows the capacity necessary "with wind." As shown, the maximum upward 2010 capacity requirement of 3500 MW occurs during HE3 (hour ending by) and HE11. Also, the maximum downward capacity requirement of 3450 MW occurs during HE24. The maximum increase in load following capacity was 800 MW which occurred during HE3 (3500 MW–2700 MW). The maximum downward capacity increase of 600 MW (3050 MW–2450 MW) occurred in HE22.

With no wind, the level of load following capacity slightly increased in 2010 above the 2006 levels due to a load growth factor of 1.5% per year. Also, the pattern of load following variation "with wind" between 2006 and 2010 is due to the unpredictability and increase in wind production between the two study years.

Fig. 14 shows the hourly load following ramping requirements due to wind only for 2010 (red arrow) compared to wind only for 2006 (green arrow). It is expected that the maximum upward load following ramping requirements in 2010 will increase by 40 MW/min (HE23: 210 MW–170 MW). Similarly,

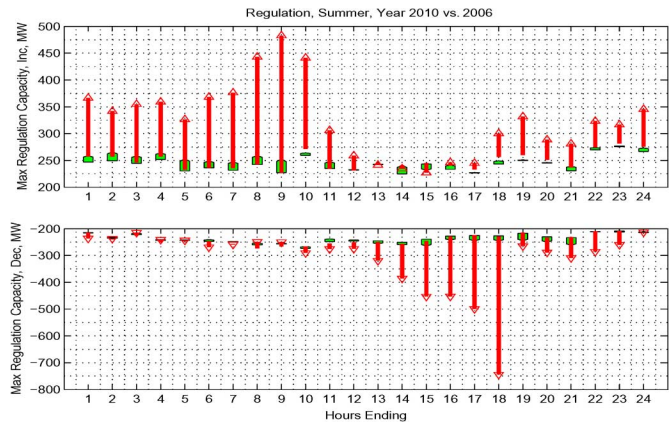

Fig. 16. Hourly capacity diagrams for regulation scenarios with wind and without wind in 2006 and 2010.

the maximum downward load following ramping requirements will increase by 40 MW/min (HE9: 180 MW–140 MW).

Fig. 15 shows the upward ramp duration is required for approximately 30 min while the downward ramp duration will be required for approximately 20 min. Overall, the upward load following capacity should be about 3500 MW and resources within the supplemental stack should be able to ramp up at a rate of about 80 MW/min for at least 30 min. Similarly, in the downward direction, the resources should be able to ramp down at a rate of approximately 175 MW/min for at least 20 min.

B. Regulation Requirement

The CAISO maintains sufficient generating capacity under AGC to continuously balance its generation and interchange schedules to its actual real-time load. Regulation is dispatched automatically through AGC every 4 s to meet minute-to-minute fluctuations in load and to correct for unintended fluctuations in generation.

As shown in Fig. 16, the regulation capacity requirement differs from the load following capacity requirement. The maximum upward 2010 regulation capacity requirement of 480 MW occurs during HE9, while the maximum downward capacity requirement of −750 MW occurs during HE18. The hourly upward increase is simply the difference between the top of the arrow and the top of the arrow for each hour. The maximum increase of 230 MW occurs during HE9 (480 MW–250 MW). The maximum downward increase of 500 MW (750 MW–250 MW) occurred in HE18.

Fig. 17 shows the hourly regulation ramping requirements due to the addition of only wind. It is expected that the maximum upward regulation ramping requirements for 2010 summer will increase by 10 MW/min (HE10: 140 MW–130 MW). The maximum downward regulation requirement in 2010 is expected to increase by 18 MW/min (HE10: 115 MW–97 MW). This is not expected to create any operational concerns because it falls within the ramping capability of the existing units. The regulation ramp duration is expected to increase by about ±10 to ±25 MW/min and could last for about 5 min.

Fig. 18 shows both the upward and downward ramp durations are required for about 5 min. Overall, the upward regulating capacity needs to be about 480 MW and resources within the sup-

Authorized licensed use limited to: Chris Mensah-Bonsu. Downloaded on April 29, 2009 at 12:58 from IEEE Xplore. Restrictions apply.

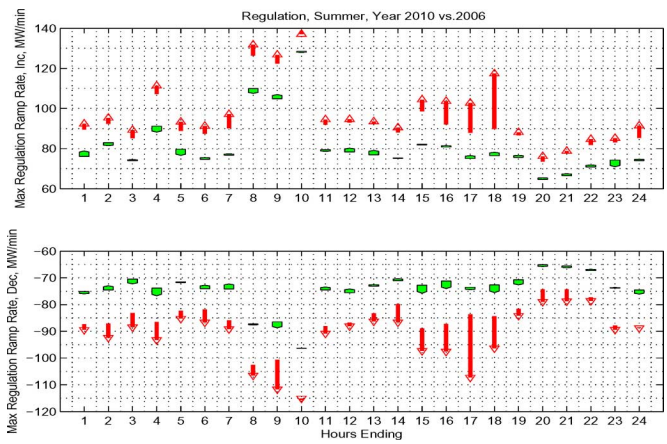

Fig. 17. Hourly ramp rate diagrams for regulation scenarios with wind and without wind in 2006 and 2010.

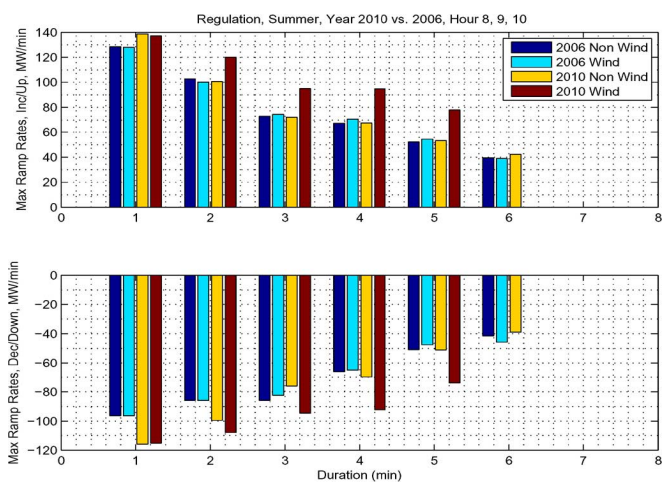

Fig. 18. Duration—ramp rates for regulation scenario (hour ending by 8, 9, and 10) with wind and without wind in 2006 and 2010.

plemental stack should be able to ramp up at a rate of about 80 MW/min for at least 5 min. Similarly, in the downward direction, the regulating capacity needs to be about −750 MW and resources should be able to ramp down at a rate of approximately 80 MW/min for at least 5 min.

VII. Conclusion

This paper presents a methodology to evaluate the impact of integrating 6700 MW of wind on the load following and regulation requirements of the CAISO Balancing Authority. The methodology is based on a mathematical model mimicking the actual CAISO's scheduling, real-time dispatch, and regulation processes and their timelines. Minute-to-minute variations and statistical interactions of the system parameters involved in these processes are depicted with sufficient details to provide a robust and accurate assessment of the additional capacity, ramping and ramp duration requirements that the CAISO regulation (AGC) and load following (ADS) systems will be facing in the year 2010. These requirements are compared to the year 2006 requirements simulated in the same way. The maximum upward 2010 load following capacity requirement is 3500 MW. Also, the downward capacity requirement is 3450 MW. The maximum increase from 2006 to 2010 is 800 MW up and 500 MW down. It is expected that the maximum upward load following ramping requirements in 2010 will increase by 40 MW/min. Similarly, the maximum downward load following ramping requirements will increase by 40 MW/min. The upward ramp duration is required for approximately 30 min while the downward ramp duration will be required for approximately 20 min. The maximum upward 2010 regulation capacity requirement is 480 MW while the maximum downward capacity requirement is 750 MW. The maximum increase is 230 MW up and 500 MW down. It is expected that the maximum upward regulation ramping requirements for 2010 summer will increase by 10 MW/min (HE10: 140 MW–130 MW). The maximum downward regulation ramping requirement in 2010 is expected to increase by 18 MW/min. This is not expected to create any operational concerns because it falls within the ramping capability of the existing units. The regulation ramp duration is expected to increase by about ±10 to ±25 MW/min and could last for about 5 min.

During the simulation, the following assumptions about input data, load and wind forecast error levels are applied. Impacts of wind generation on the interconnection frequency are neglected. The hour-ahead load and wind generation energy forecasts are provided the latest 120 min before the actual beginning of an operating hour. The real-time 5-min load forecasts are provided 7.5 min before the actual beginning of a 5-min dispatch interval (or 10 min before the middle point of this interval). The load forecast errors are unbiased (i.e., they have negligible average), and will have the same distribution in 2010 as it had in 2006. The load and wind forecast errors are random variables distributed according the truncated normal distribution with certain autocorrelation between the subsequent forecast errors. Wind generation forecasts are not biased over a season. Wind generation schedules are solely based on the corresponding hour-ahead wind generation forecasts that assumed to be available for the ISO/IOU scheduling process.

The proposed methodology can find application in balancing authorities, utilities, project developments and government organizations (RPS developers) to evaluate more accurately the impact of wind generation on the grid balancing generation requirements. For example, this methodology has been used by Bonneville Power Administration (BPA) to develop its rate case methodology and to evaluate the expected impacts of wind generation on their load following and regulation requirements [31]. Currently, the methodology forms a base in the BPA/DOE project "Simulation Model for the Comprehensive Analysis of Expected Wind Generation Development Scenarios in the Pacific Northwest and Their Impacts on the Power Grid Operations".

Acknowledgment

The authors would like to thank Mr. Y. Mansour, President and CEO of the CAISO; Mr. A. Perez, VP of Planning and Infrastructure Development (P&ID); J. Detmers, VP of Operations; and G. DeShazo, Director in P&ID for their interest and support throughout this project. The CAISO engineers, dispatchers, and consultants, including D. Hawkins, S. Chowdhury, T. VanBlaricom, T. Yong, H. Alarian, J. Blatchford, and T. Wu, helped

Authorized licensed use limited to: Chris Mensah-Bonsu. Downloaded on April 29, 2009 at 12:58 from IEEE Xplore. Restrictions apply.

to better understand CAISO operating practices and verify the study results. J. Zack and M. Brower (AWS Truewind Company) assisted in developing the wind power production and forecast models. B. McManus, S. Burton, and J. Murthy (Bonneville Power Administration) participated in productive meetings discussing some details of this methodology.

REFERENCES

[1] M. J. Grubb, "The integration of renewable electricity sources," *Energy Policy*, vol. 19, pp. 670–688, Sep. 1991.

[2] N. Hatziargyriou and A. Zervos, "Wind power development in Europe," *Proc. IEEE*, vol. 89, no. 12, pp. 1765–1782, Dec. 2001.

[3] B. Parsons, M. Milligan, B. Zavadil, D. Brooks, B. Kirby, K. Dragoon, and J. Caldwell, "Grid impacts of wind power: A summary of recent studies in the United States," *Wind Energy*, vol. 7, pp. 87–108, 2004.

[4] J. C. Smith, M. R. Milligan, E. A. DeMeo, and B. Parsons, "Utility wind integration and operating impact state of the art," *IEEE Trans. Power Syst.*, vol. 22, no. 3, pp. 900–908, Aug. 2007.

[5] Y. Wan and J. R. Liao, "Analyses of wind energy impact on WFEC system operations," in *Proc. Eur. Wind Energy Conf.*, Athens, Greece, Feb. 27–Mar. 2, 2006.

[6] M. Milligan and B. Kirby, "Impact of balancing areas size, obligation sharing, and ramping capability on wind integration," in *Proc. WindPower 2007 Conf. Exhib.*, Los Angeles, CA, Jun. 3–6, 2007.

[7] D. Brooks, E. Lo, R. Zavadil, S. Santoso, and J. Smith, Characterizing the Impacts of Significant Wind Generation Facilities on Bulk Power System Operations Planning, May 2003, Xcel Energy—North Case Study, Fin. Rep.

[8] B. W. Kennedy, "Integration wind power transmission and operational impacts," in *Proc. reFOCUS*, Jan./Feb. 2004, pp. 36–37.

[9] G. Majstrovic and D. Bajs, "Impact of wind power plants on Croatian power system operation," in *Proc. Int. Conf. Clean Electric Power*, Capri, Italy, May 21–23, 2007.

[10] M. D. Ilic, Y. V. Makarov, and D. Hawkins, "Operations of electric power systems with high penetration of wind power: Risks and possible solutions," in *Proc. IEEE PES General Meeting, 2007*, Tampa, FL, Jun. 24–28, 2007.

[11] E. A. DeMeo, W. Grant, M. R. Milligan, and M. J. Schuerger, "Wind plant integration, costs, status, and issues," *IEEE Power Energy Mag.*, vol. 3, no. 6, pp. 38–46, Nov./Dec. 2005.

[12] D. L. Brooks, E. O. Lo, J. W. Smith, J. H. Pease, and M. McGree, Assessing the Impact of Wind Generation on System Operations at XCEL Energy—North and Bonneville Power Administration. [Online]. Available: http://www.uwig.org/opimpactspaper.pdf. pp. 1–15

[13] G. Strbac, A. Shakoor, M. Black, D. Pudjianto, and T. Bopp, "Impact of wind generation on the operation and development of the UK electricity systems," *Elect. Power Syst. Res.*, vol. 77, pp. 1214–1227, 2007.

[14] S. Persaud, B. Fox, and D. Flynn, "Modelling the impact of wind power fluctuations on the load following capability of an isolated thermal power system," *Wind Eng.*, vol. 24, no. 6, pp. 399–415, 2000.

[15] S. Persaud, B. Fox, and D. Flynn, "Effects of large scale wind power on total system variability and operation: Case study of Northern Ireland," *Wind Eng.*, vol. 27, p. 320, 2003.

[16] B. C. Ummels, M. Gibescu, E. Pelgrum, W. L. Kling, and A. J. Brand, "Impacts of wind power on thermal generation unit commitment and dispatch," *IEEE Trans. Energy Convers.*, vol. 22, no. 1, pp. 44–51, Mar. 2007.

[17] P. Sørensen, N. A. Cutululis, A. Vigueras-Rodríguez, L. E. Jensen, J. Hjerrild, M. H. Donovan, and H. Madsen, "Power fluctuations from large wind farms," *IEEE Trans. Power Syst.*, vol. 22, no. 3, pp. 958–965, Aug. 2007.

[18] H. Holttinen, "Impact of hourly wind power variations on the system operation in the Nordic countries," *Wind Energy*, vol. 8, pp. 197–218, 2005.

[19] B. C. Ummels, M. Gibescu, W. L. Kling, and G. C. Paap, "Integration of wind power in the liberalized Dutch electricity market," *Wind Energy*, vol. 9, pp. 579–590, 2006.

[20] B. Kirby and E. Hirst, Customer-Specific Metrics for the Regulation and Load-Following Ancillary Services, Oak Ridge National Laboratory, Jan. 2000.

[21] Analysis of Wind Generation Impact on ERCOT Ancillary Services Requirements, General Electric Company (GE), Mar. 28, 2008, Technical Report.

[22] California Renewables Portfolio Standard Renewable Generation Integration Cost Analysis: Multi-Year Analysis Results and Recommendations, California Energy Commission, Fin. Rep. CEC-500-2006-064, Jun. 2006. [Online]. Available: http://www.energy.ca.gov/2006publications/CEC-500-2006-064/CEC-500-2006-064.PDF.

[23] Intermittency Analysis Project: Appendix B Impact of Intermittent Generation on Operation of California Power Grid, California Energy Commission Report CEC-500-2007-081-APB, Jul. 2007. [Online]. Available: http://www.energy.ca.gov/2007publications/CEC-500-2007-081/CEC-500-2007-081-APB.PDF.

[24] Y. V. Makarov and D. L. Hawkins, "Quantifying the impact of wind energy on power system operating reserves," in *Proc. Global Windpower Conf. Exhib.*, Chicago, IL, Mar. 28–31, 2004.

[25] CAISO Market Simulation Guidebook, Jul. 25, 2008. [Online]. Available: http://www.caiso.com/18d3/18d3d1c85d730.pdf.

[26] Y. V. Makarov, J. Blatchford, H. Alarian, K. DeMarse, M. O'Hara, M. Scholz, S. Jercich, J. Vidov, E. Leuze, R. Abernathy, D. L. Hawkins, and J. Zack, "Incorporation of wind power resources into the California energy market," in *Proc. WINDPOWER Conf. Exhib. 2005*, Denver, CO, May 15–18, 2005.

[27] D. L. Hawkins, J. Blatchford, and Y. V. Makarov, "Wind integration issues and solutions in California," in *Proc. IEEE PES General Meeting*, Tampa, FL, Jun. 24–28, 2007.

[28] *Real Power Balancing Control Performance*, NERC Std. BAL-001-0, Apr. 1, 2005.

[29] D. C. Barr, "The use of a data historian to extend plant life," in *Proc. Int. Conf. Life Management of Power Plants*, U.K., Dec. 12–14, 1994, Heriot-Watt Univ..

[30] T. S. Nielsen, A. Joensen, H. Madsen, L. Landberg, and G. Giebel, "A new reference for wind power forecasting," *Wind Energy*, vol. 1, pp. 29–34, 1998.

[31] Y. V. Makarov, S. Lu, B. Mcmanus, and J. Pease, "The future impact of wind on BPA power system ancillary services," in *Proc. IEEE Transmission and Distribution Conf.*, Chicago, IL, Apr. 2008.

Yuri V. Makarov (SM'99) received the M.Sc. degree in computers and the Ph.D. degree in electrical engineering from the Leningrad Polytechnic Institute (now St. Petersburg State Technical University), Leningrad, Russia.

From 1990 to 1997, he was an Associate Professor in the Department of Electrical Power Systems and Networks at St. Petersburg State Technical University. From 1993 to 1998, he conducted research at the University of Newcastle, University of Sydney, Australia, and Howard University, Washington, DC. From 1998 to 2000, he worked at the Transmission Planning Department, Southern Company Services, Inc., Birmingham, AL, as a Senior Engineer. From 2001 to 2005, he occupied a senior engineering position at the California Independent System Operator, Folsom, CA. Now he works for the Pacific Northwest National Laboratory (PNNL), Richland, WA. His activities are around various theoretical and applied aspects of power system analysis, planning, and control. He participated in many projects concerning power system transmission planning (power flow, stability, reliability, optimization, etc.) and operations (control performance criteria, quality, regulation, impacts of intermittent resources, etc.).

Dr. Makarov was a member of the California Energy Commission Methods Group developing the Renewable Portfolio Standard for California; a member of the Advisory Committee for the EPRI/CEC project developing short-term and long-term wind generation forecasting algorithms; and a voting member of the NERC Resources Subcommittees and NERC Wind Generation Task Force. For his role in the NERC August 14th Blackout Investigation Team, he received a Certificate of Recognition signed by the U.S. Secretary of Energy and the Minister of Natural Resources, Canada.

Authorized licensed use limited to: Chris Mensah-Bonsu. Downloaded on April 29, 2009 at 12:58 from IEEE Xplore. Restrictions apply.

Clyde Loutan (SM'06) received the B.S. degree and the M.S. degree in electrical engineering from Howard University, Washington DC.

He worked for Pacific Gas and Electric Company for 14 years in various capacities such as real-time system operations, transmission planning, and high voltage protection. For over a year, he consulted with Ecco International, Inc. before joining the CAISO in 2000. In his current position, he focuses on system operation performance-related issues. He has been instrumental in developing several policies at the CAISO and was the lead engineer in charge of investigating the root cause of the California blackouts in 2000 and 2001. He was the team lead for integrating the first pseudo tie to operate within the CAISO market construct and is currently the project lead for renewables integration at the CAISO. He is also on the WECC Minimum Operating Reliability Council work team, which is responsible for setting reliability standards for the Western Interconnection and is on several NERC drafting teams working on developing national control performance standards.

Mr. Loutan is a registered Professional Engineer.

Jian Ma (M'08) received the B.S. degree from Shandong University, Jinan, China, in 1996, the M.S. degree from Dalian University of Technology, Dalian, China, in 1999, and the Ph.D degree in electrical engineering from The University of Queensland, Brisbane, Australia, in 2008.

He worked as a Senior Programmer and Research Engineer at electric power R&D companies in China, focusing mainly on EMS/SCADA/DTS, and he was a research associate at the School of Mechanical and Aerospace Engineering at Nanyang Technological University, Singapore. He is currently a research engineer at Pacific Northwest National Laboratory (PNNL), Richland, WA. His research interests include power system stability and control, power system security assessment, artificial intelligence application in power systems, and wind power integration into power systems.

Phillip de Mello (S'07) received the B.S. degree in mechanical engineering from the University of Connecticut, Storrs, in 2005, and the M.S. degree in mechanical and aeronautical engineering from University of California at Davis in 2007. He is currently pursuing the Ph.D. degree in mechanical and aeronautical engineering at the University of California at Davis.

Since 2006, he has been an Engineering Intern at the California Independent System Operator. He has worked on the design and analysis of electricity markets. Currently, his work and research interest include integration of renewable resources, particularly the effects of intermittent resources on the power grid and electricity markets.

Authorized licensed use limited to: Chris Mensah-Bonsu. Downloaded on April 29, 2009 at 12:58 from IEEE Xplore. Restrictions apply.